3-Methyl-4-amino-5-mercapto-1,2,4-triazole as corrosion inhibitor for 6061/Al - 15 (vol -%) SiC$_{(p)}$ composite in 0.5 M sodium hydroxide solution

Reena Kumari P. D.[1], Jagannath Nayak [2], A. Nityananda Shetty [3*]

[1]Department of Chemistry, Srinivas School of Engineering, Mukka, Mangalore -575 025, Karnataka, India
[2]Department of Metallurgical & Materials Engineering, National Institute of Technology Karnataka, Surathkal, Srinivasnagar – 575 025, Karnataka, India
[3]Department of Chemistry, National Institute of Technology Karnataka, Surathkal, Srinivasnagar – 575 025, Karnataka, India

[*]Corresponding author: E-mail address: nityashreya@gmail.com; Tel: +91-824-2474200, +91-9448779922; Fax: +91-824-2474033,

Abstract

3-Methyl-4-amino-5-mercapto-1,2,4-triazole (MAMT) was investigated for its inhibition action on the corrosion of 6061/Al - 15 (vol-%) SiC$_{(p)}$ composite in 0.5 M sodium hydroxide solution at different temperatures by potentiodynamic polarization and electrochemical impedance spectroscopic techniques. The effect of inhibitor concentration, temperature and concentration of the corrosion medium on the inhibitor action was investigated. The inhibition efficiency increased with the increase in the concentration of inhibitor but decreased with the increase in temperature. Both thermodynamic and activation parameters were calculated and discussed. The adsorption of MAMT on the composite was found to be through physisorption obeying Langmuir's adsorption isotherm.

Key words: Maraging steel, EIS, SEM, adsorption, corrosion inhibition

1. Introduction

Metal matrix composites, especially with aluminum alloy matrices, have found widespread use in many engineering applications because of their high-strength-to weight ratio. The high thermal conductivity and low coefficients of thermal expansion of these materials have lead to a number of applications in military, automobile and aerospace fields [1-3]. One of the main obstacles to the widespread incorporation of particulate MMCs into engineering applications is the influence of reinforcements on corrosion resistance. This is of particular importance in aluminum alloy based composites where corrosion resistance is imparted by a protective oxide film. The addition of a reinforcing phase could lead to discontinuities or flaws in the film, increasing the sites for corrosion initiation and thereby rendering the composite liable to severe attack [4].

The use of inhibitors is one of the most common methods to protect metallic materials against corrosion in aggressive corrosion environments. The high corrosion rate of the composite materials in alkaline and acidic media can be combated by using organic inhibitors. It has been reported that many organic compounds containing hetero atoms like N, O, S, and multiple bonds in their molecules have been proved to be effective inhibitors for the corrosion of aluminum alloys in acid and alkaline media [5-9]. The action of inhibitors in aggressive media is assumed to be by the adsorption of the inhibitor molecules onto the metal surface. The processes of adsorption of inhibitors are influenced by the nature and surface charge of the metal, the chemical structure of organic inhibitors, the type of aggressive electrolyte and the type of interaction between organic molecules and the metallic surface [10]. Our research group has earlier reported 4-(N,N-dimethylamino)benzaldehyde thiosemicarbazone and 3-methyl-4-amino-5-mercapto-1,2,4-triazole as inhibitors for the corrosion of 6061/Al - 15 (vol-%) $SiC_{(p)}$ composite in acid medium and 6061 Al alloy in alkaline medium, respectively [11, 12].

1,2,4-triazoles and their derivatives are incorporated into a wide variety of therapeutically important compounds possessing a broad spectrum of biological activities and many other applications including corrosion inhibition of metals[13,14]. These compounds can be adsorbed on the metal surface through lone pairs of electrons on nitrogen or sulfur atoms and also through pi electrons present in these molecules [15]. From the literature survey it is evident that, there is no published information available on triazole derivatives as corrosion inhibitors for the

aluminum composite material in alkaline media. The present study is at investigating the potential of 3-methyl-4-amino-5-mercapto-1,2,4-triazole (MAMT) as corrosion inhibitor for 6061/Al - 15 (vol-%) $SiC_{(p)}$ composite in 0.5 M sodium hydroxide solution using potentiodynamic polarization and electrochemical impedance techniques. The effects of temperature, inhibitor concentration, immersion time were also studied.

2. Experiemental

2.1. Materials
The material employed was 6061/Al - 15 (vol-%) $SiC_{(p)}$ composite in extruded rod form (extrusion ratio 30:1). The chemical composition of the base metal 6061 aluminum alloy is given in Table 1.The composite is made of 6061 Al base alloy reinforced with particulate SiC (99.9% purity) and 23 μm size. The sample was metallographically mounted up to 10 mm height using cold setting epoxy resin, so that the exposed surface area of the metal to the media is 0.95 cm^2. These coupons were polished as per standard metallographic practice-belt grinding followed by abrading on emery papers of 400, 600, 800, 1000, 1200 and 1500 grades, finally on polishing wheel using levigated alumina to obtain mirror finish – degreased with acetone, washed with double distilled water, and dried before immersing in the corrosion medium.

Table 1 The chemical composition of the base metal 6061 aluminum alloy

| Element	Cu	Si	Mg	Cr	Al
Composition (wt %)	0.25	0.6	1.0	0.25	Balance

2.2. Medium
The test solution used for the investigation, solution of 0.5 M sodium hydroxide was prepared by using sodium hydroxide pellets of AR grade and double distilled water and the solution was

standardized. Experiments were carried out using calibrated thermostat at temperatures 30 ^{o}C, 35 ^{o}C, 40 ^{o}C, 45 ^{o}C and 50 ^{o}C (±0.5 ^{o}C). Inhibitive action of MAMT on the corrosion of Al-SiC composite in 0.5 M NaOH solution was studied by

J. Mater. Environ. Sci. 2 (4) (2011) 387-402
ISSN : 2028-2508

Kumari et al.

introducing different concentrations of the inhibitor into the solution at five different temperatures.

2.3. Synthesis of MAMT
3-Methyl-4-amino-5-mercapto-1,2,4-triazole was synthesized and re-crystallized as per the reported procedure in one step reaction of thiocarbohydrazide and glacial acetic acid [16]. A mixture of thiocarbohydrazide (10 g) and acetic acid (60 ml) was taken in a round bottomed flask. The reaction mixture was refluxed for about 4 h. The precipitated product was purified by recrystallization from hot water and was identified by melting point (203 – 204 ^{o}C), elemental analysis and infrared spectra. The molecular weight of the compound is 130. The structure of the molecule is shown below.
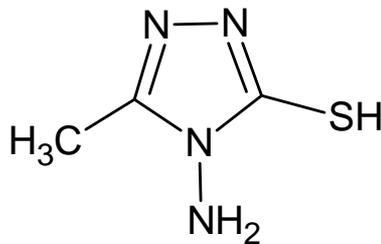
2.3. Electrochemical measurements
Electrochemical measurements were carried out by using electrochemical work station, Gill AC and ACM Instruments Version 5 software. The measurements were carried out using conventional three electrode Pyrex glass cell with platinum counter electrode and saturated calomel electrode (SCE) as reference electrode. All the values of potential are therefore referred to the SCE. In potentiodynamic polarization (Tafel) method, the finely polished composite specimens were exposed to corrosion medium of sodium hydroxide in the absence and presence of inhibitor at different temperatures (30° C - 50 ^{o}C) and allowed to establish a steady state open circuit potential (OCP). The potentiodynamic current-potential curves (Tafel plots) were recorded by polarizing the specimen to -250 mV cathodically and +250 mV anodically with respect to OCP at a scan rate of 1 mV s^{-1}.

In EIS technique a small amplitude ac signal of 10 mV and frequency spectrum from 100 kHz to 0.01 Hz was impressed at the OCP and

impedance data were analyzed using Nyquist plots.

In all the above measurements, at least three similar results were considered and their average values are reported.

2.4. Scanning electron microscopy (SEM) analysis
The scanning electron microscope images of the samples were recorded using JEOL JSM – 6380 LA analytical scanning electron microscope.

3. Results and discussion

3.1. Potentiodynamic polarization (PDP) measurements
Fig.1. shows the Tafel polarization curves for the corrosion of the composite in 0.5 M NaOH solution at 30 ^{o}C in the presence of different concentrations of MAMT. Similar results were obtained at other temperatures also.
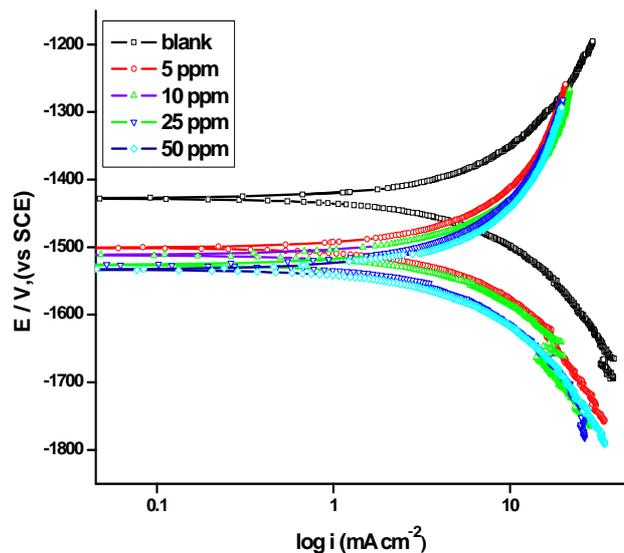
Figure 1. Tafel polarization curves for the corrosion of 6061/Al - 15 (vol-%) SiC$_{(p)}$ composite in 0.5 M NaOH at 30 ^{o} C in the presence of different concentrations of MAMT.

Inhibition efficiency (η) was calculated using expression (1).

$$\eta = \frac{i_{corr_{(uninh)}} - i_{corr_{(inh)}}}{i_{corr_{(uninh)}}} \times 100 \qquad (1)$$

where $i_{corr(uninh)}$ and $i_{corr(inh)}$ are the corrosion current densities in the absence and presence of the

inhibitor, respectively. The corrosion rate is calculated using the Eq. 2:

$$v_{corr} \ (mm \ y^{-1}) = \frac{3270 \times M \times i_{corr}}{\rho \times Z} \qquad (2)$$

where 3270 is a constant that defines the unit of corrosion rate, i_{corr} is the corrosion current density in A cm^{-2} , ρ is the density of the corroding material, (g cm^{-3}), M is the atomic mass of the metal, and Z is the number of electrons transferred per atom [17].

The electrochemical parameters including corrosion potential (E_{corr}), corrosion current density (i_{corr}), corrosion rate (v_{corr}), anodic and cathodic slopes (b_a and b_c), and inhibition efficiency (η) were calculated from Tafel plots, and are summarized in Table 2. As can be seen from the data, addition of MAMT decreases the corrosion rate of the composite sample. Inhibition efficiency increases with the increase in MAMT concentration. The changes in both the anodic and

cathodic Tafel slopes observed on the addition of MAMT indicate both anodic and cathodic reactions are affected by the addition of inhibitor. It is also seen that the addition of MAMT shifts the E_{corr} values toward more negative potential, indicating a predominant cathodic inhibition action by MAMT. According to Ferreir et al and Li et al [18, 19] if the displacement in corrosion potential is more than ± 85 mV with respect to the corrosion potential of the blank, the inhibitor can be considered as a distinctive cathodic or anodic type. The magnitudes of shift in E_{corr} values observed indicate that MAMT is a predominant cathodic type inhibitor. The change in the values of b_c in the presence of the inhibitor indicates the influence of the compound on the kinetics of cathodic reaction. The shift in the anodic Tafel slope b_a may be due to the inhibitor molecules adsorbed on the composite metal surface, affecting the dissolution of the metal [20].
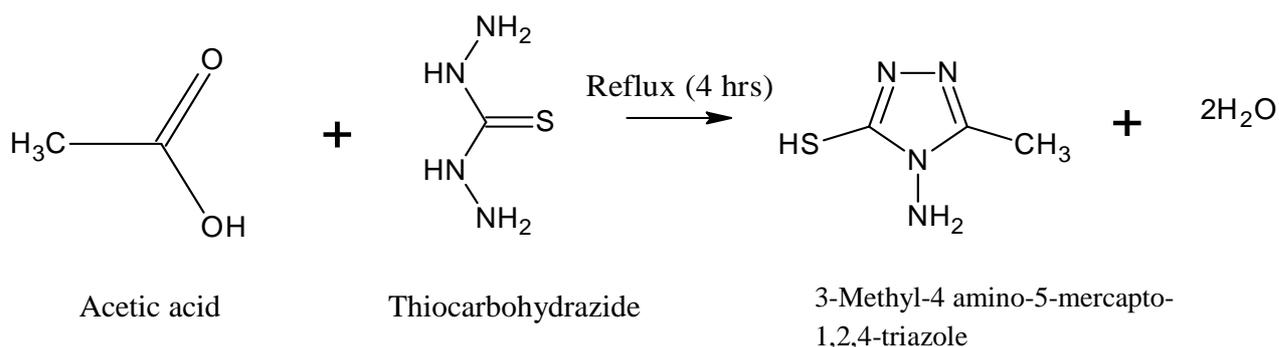
Scheme 1 Synthesis of 3-methyl-4 amino-5-mercapto-1,2,4-triazole

3.2. Electrochemical impedance spectroscopy (EIS) studies

The Nyquist plots obtained for the corrosion of 6061/Al - 15 (vol-%) SiC$_{(p)}$ composite in 0.5 M NaOH containing different concentrations of MAMT are as shown in Fig. 2. As can be seen from Fig. 2, the impedance diagrams show semicircles, indicating that the corrosion process is mainly charge transfer controlled and the addition of MAMT does not

change the reaction mechanism of the corrosion of composite in sodium hydroxide solution. These results support the results of polarization measurements that the inhibitor does not alter the mechanism of electrochemical reactions responsible for the corrosion. It inhibits the corrosion primarily through its adsorption and subsequent formation of a barrier film on the metal surface [21].

Table 2 Electrochemical parameters from Tafel polarization studies for the corrosion of 6061/Al - 15 (vol-%) $SiC_{(p)}$ composite in 0.5 M NaOH solution containing different concentrations of MAMT.

Temp (°C)	Inhibitor concentration (ppm)	E_{corr} (mV/SCE)	b_a (mV dec^{-1})	$-b_c$ (mV dec^{-1})	i_{corr} (mA cm^{-2})	υ_{corr} (mm y^{-1})	η (%)
30	0	-1428	460	405	9.95	106.81	-
	5	-1501	243	201	4.30	46.07	56.8
	10	-1511	200	182	3.93	42.23	60.5
	25	-1526	204	190	3.32	36.37	65.9
	50	-1534	160	149	2.94	31.46	70.5
35	0	-1466	490	359	10.60	113.87	-
	5	-1494	190	172	4.60	49.21	56.7
	10	-1513	205	212	4.23	45.36	60.1
	25	-1528	199	168	3.63	38.85	65.8
	50	-1537	237	227	3.27	35.06	69.1
40	0	-1470	425	419	10.86	116.62	-
	5	-1496	237	202	4.98	53.35	54.1
	10	-1517	189	181	4.50	48.21	58.5
	25	-1533	182	200	3.98	42.63	63.3
	50	-1543	158	148	3.81	40.78	64.9
45	0	-1476	447	420	11.43	122.76	-
	5	-1489	214	242	5.27	56.40	53.9
	10	-1511	192	216	4.81	51.49	57.9
	25	-1535	159	153	4.30	46.02	62.4
	50	-1541	259	198	4.17	44.66	63.5
50	0	-1471	474	419	11.81	126.46	-
	5	-1488	175	183	5.58	59.81	52.7
	10	-1493	216	206	5.25	56.28	55.5
	25	-1535	201	196	4.64	49.70	60.7
	50	-1550	266	208	4.61	49.35	61.0

The impedance plots consist of two capacitive semicircles, separated by a small inductive loop at intermediate frequencies. The high frequency capacitive loop could be assigned to the charge transfer of the corrosion process and to the formation of oxide layer [22, 23]. Due to the ionic conduction in the film, the oxide film is considered to be a parallel circuit of a resistor and due to its dielectric properties, as a capacitor. The capacitive loop is due to the interfacial reactions, particularly, the reaction of aluminum oxidation at the metal/oxide/electrolyte interface [24, 25]. The process includes the formation of Al$^+$ ions at the metal/oxide interface, and their migration through the oxide/solution interface where they are oxidized to Al^{3+}. At the oxide/solution interface, OH$^-$ or O^{2-} ions are also formed. The fact that all the three processes are represented by only one loop could be attributed either to the overlapping of the loops of the processes, or to the assumption that one process dominates over the others and, therefore, excludes the other processes [26]. The inductive loop may be related to the relaxation process obtained by the adsorption/ incorporation of charged intermediates on and into the oxide film [27, 28]. Low frequency capacitive loop indicated the growth and dissolution of the surface film

J. Mater. Environ. Sci. 2 (4) (2011) 387-402
ISSN : 2028-2508

Kumari et al.
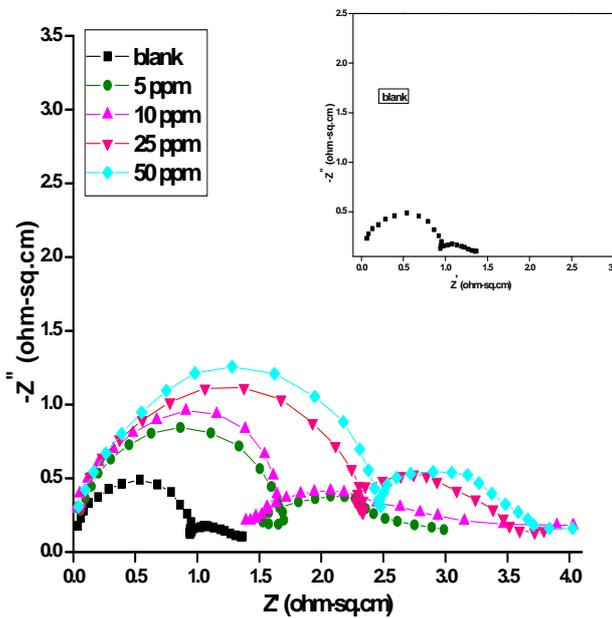
Figure 2. Nyquists plots for the corrosion of 6061/Al - 15 (vol-%) $SiC_{(p)}$ composite in 0.5 M NaOH at 30 °C in the presence of different concentrations of MAMT.

The impedance data were analyzed using an equivalent circuit (EC) that tentatively models the physical processes occurring at the metal-electrolyte interface using ZSimpWin software of version 3.21. The proposed EC represents two distinct components of the protective films on the composite surface with an oxide layer and an adsorbed inhibitor layer on it. The EC consists of six elements as shown in Fig. 3. In this equivalent circuit, R_s is the solution resistance and L represents an inductive element. This also consists of two R_1-Q_1 and R_2-Q_2 terms in series with L and R_s.

The semicircles of the impedance spectra for the composite in the presence of the inhibitor are depressed. Deviation of this kind is referred to as frequency dispersion, and has been attributed to inhomogeneities of solid surfaces [29]. The inhomogeneity in the composite is expected as the alloy is reinforced with SiC particles. An exponent n in the impedance function has been suggested as a deviation parameter from the ideal behavior [22, 23]. By this suggestion, the capacitor in the equivalent circuit can be replaced by a so-called

constant phase element (CPE), which is a frequency-dependent element and related to surface roughness. The impedance function of a CPE has the following equation [27]:

$$Z_{CPE} = Y_o^{-1}(j\omega)^{-n} \tag{3}$$

where the amplitude Y_0 and n are frequency independent CPE constant and exponent, respectively, and ω is the angular frequency in rad s^{-1} for which $-Z''$ reaches its maximum value, and $j^2 = -1$, an imaginary number. n is dependent on the surface morphology, with values, $-1 \leq n \leq 1$. Y_0 and n can be calculated by the equations proved by Mansfeld et al [30].

In the absence of inhibitors the semicircle of the impedance spectra is more or less not depressed (shown in the inset of Fig 2) and this can be due to the high corrosion rate of the composite in NaOH solution. In the highly alkaline solution, the corrosion rate of aluminum is so high that it almost undergoes uniform corrosion and therefore, the surface inhomogeneity does not affect the Nyquist plot. In the presence of inhibitor, with the progressive formation of the surface layer of inhibitor, the corrosion rate decreases and surface no more remains uniform and homogeneous. Therefore, the effect of surface inhomogeneity comes into effect in depressing the semicircles of the Nyquist plots. The double layer capacitances C_{dl}, for a circuit including CPE were calculated from the following equation [31]:

$$C_{dl} = Y_o (2\pi f_{max})^{n-1} \tag{4}$$

where f_{max} is the frequency at which the imaginary component of the impedance is maximal. According to the expression of the double layer capacitance presented in the Helmholtz model [20]:

$$C_{dl} = \frac{\varepsilon\varepsilon_o}{d} S \tag{5}$$

where d is the thickness of the film, S is the surface area of the electrode, ε_0 is the permittivity of air and ε is the local dielectric constant.
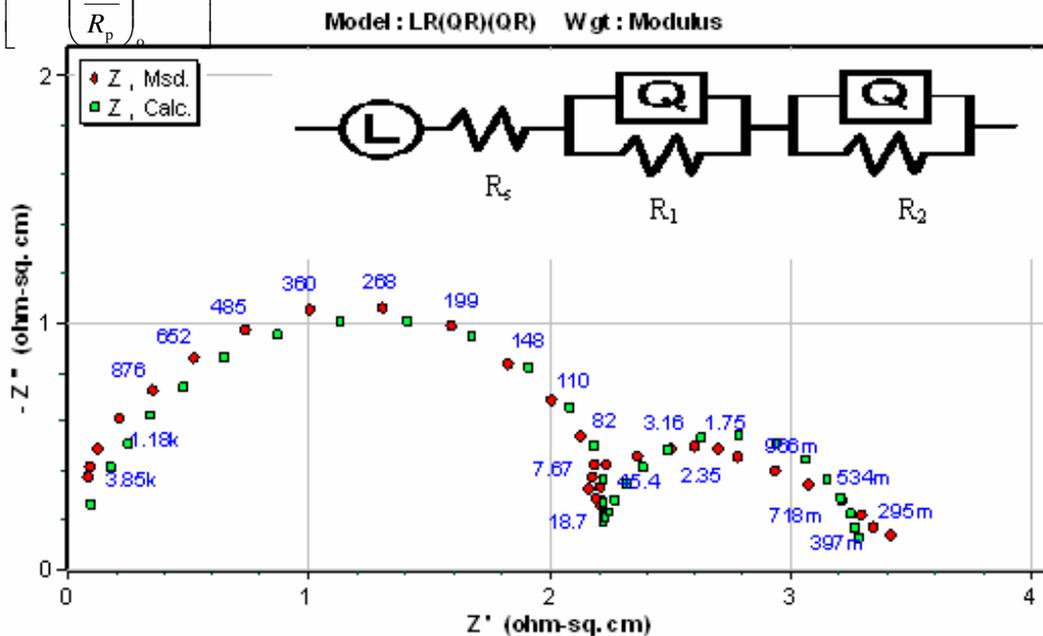
In accordance with the EC given in Fig. 3, the polarization resistance, R_p can be calculated from Eq. (6):

$$R_p = R_1 + R_2 \tag{6}$$

The inhibition efficiency (η) , was calculated from the following equation.

$$\eta = \left[\frac{\left(\frac{1}{R_p}\right)_o - \left(\frac{1}{R_p}\right)}{\left(\frac{1}{R_p}\right)_o} \right] \times 100 \qquad (7)$$

where $(R_p)_o$ and (R_p) are the uninhibited and inhibited polarization resistances, respectively.

Figure 3. The equivalent circuit model used to fit the EIS experimental data of the composite (in the presence of 25 ppm MAMT).

The EIS data for the corrosion of 6061/Al - 15 (vol-%) SiC$_{(p)}$ composite in 0.5 M NaOH in the presence of different concentrations of MAMT are given in Table 3. The measured values of polarization resistance (R_p) increase and that of the double layer capacitance (C_{dl}) decrease with the increasing concentration of MAMT in the solution, indicating the decrease in the corrosion rate for the composite with increase in MAMT concentration. This is in accordance with the observations obtained from Tafel measurements. The value of C_{dl} decreases due to the adsorption of inhibitor molecules, which displaces water molecules originally adsorbed on the alloy surface and decreases the active surface area. The value of double layer capacitance decreases with the increase in inhibitor concentration indicating that inhibitor molecules function by adsorption at the metal/ solution interface, leading to protective film

on the alloy surface, and decreasing the extent of dissolution reaction [32].

3.3. Effect of Temperature

The effect of temperature on the inhibited electrolyte-metal reaction is highly complex because many changes occur on the metal surface, such as desorption of the inhibitor molecules, which in some cases may undergo decomposition and/or rearrangement [33]. However the study of temperature effect facilitates the calculation of many thermodynamic parameters for the inhibition and/ or the adsorption processes which contribute to determine the type of inhibition and/ or adsorption of the studied inhibitors. In the present study, with the increase in solution temperature, corrosion current density (i_{corr}) and hence the corrosion rate of the specimen increased in both the blank and inhibited solutions. The inhibition

efficiency decreases with the increase in temperature. This may be attributed to the higher dissolution rates of the aluminum composite at higher temperatures. This may also be due to a possible desorption of the adsorbed inhibitor due to increased solution agitation resulting from higher rates of gas evolution, which may also reduce the ability of the inhibitor to be adsorbed on the metal surface [34]. Such a behavior suggests physical adsorption of the MAMT on the corroding aluminum surface [10].

The apparent activation energy (E_a) for the corrosion process in the presence and absence of inhibitor can be calculated using Arrhenius law Eq 8.

$$\upsilon_{corr} = k \exp\left(\frac{-E_a}{RT}\right) \tag{8}$$

where k is the Arrhenius pre-exponential factor, R is the universal gas constant and T is the absolute temperature. The plot of ln (υ_{corr}) versus reciprocal of absolute temperature $1/T$ gives a straight line whose slope is equal to $-E_a/R$, gives the activation energy for the corrosion process. The Arrhenius plots for the corrosion of composite specimens in the presence of different concentrations of MAMT in 0.5 M NaOH are shown in Fig. 4.

The entropy and enthalpy of activation values for the dissolution of composite (ΔH_a and ΔS_a) were calculated from the transition state theory Eq 9.

$$\upsilon_{corr} = \frac{RT}{Nh} \exp\left(\frac{\Delta S_a}{R}\right) \exp\left(\frac{-\Delta H_a}{R}\right) \tag{9}$$

where h is Planck's constant, N is Avogadro's number. A plot of ln (υ_{corr}/T) versus $1/T$ gives a straight line with slope equal to $-\Delta H_a/R$ and intercept equal to $\ln(R/Nh) + \Delta S_a/R$. The plots of $\ln(\upsilon_{corr}/T)$ versus $1/T$ for the corrosion of composite samples in the presence of different concentrations of MAMT in 0.5 M NaOH are shown in Fig. 5. The calculated values of the apparent activation energy E_a, activation enthalpy ΔH_a, and activation entropy ΔS_a are given in Table 4.
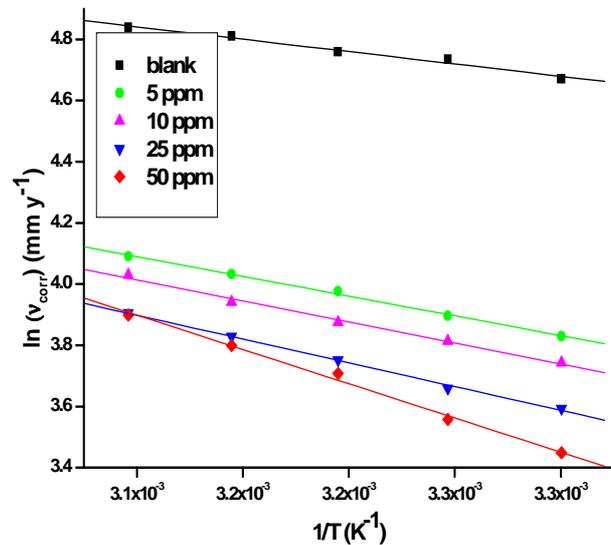
Figure 4. Arrehnius plots for the corrosion of 6061/Al-15 (vol-%) SiC$_{(p)}$ composite in 0.5 M NaOH in the presence of different concentrations of MAMT.
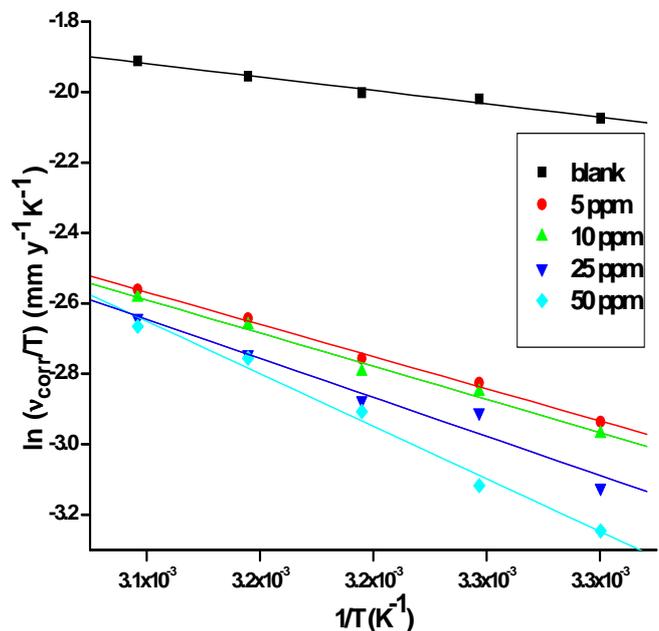
Figure 5. ln (υ_{corr}/T) vs. $1/T$ plots for the corrosion of 6061/Al - 15 (vol-%) SiC$_{(p)}$ composite in 0.5 M NaOH in the presence of different concentrations of MAMT.

Table 3. EIS data for the corrosion of 6061/Al - 15 (vol-%) SiC$_{(p)}$ composite in 0.5 M NaOH solution containing different concentrations of MAMT.

Temp (^{o}C)	Inhibitor concentration (ppm)	R_p (ohm cm^2)	C_{dl} (F cm^{-2})	η (%)
	0	1.7	0.30	-
	5	3.8	0.18	55.4
30	10	4.2	0.16	59.5
	25	4.7	0.15	63.8
	50	4.8	0.14	64.6
	0	1.6	0.37	-
	5	3.4	0.20	54.2
35	10	3.7	0.17	56.0
	25	4.3	0.16	63.2
	50	4.4	0.15	63.6
	0	1.5	0.44	-
	5	3.1	0.31	50.8
40	10	3.3	0.18	54.8
	25	3.9	0.17	62.3
	50	4.0	0.16	63.1
	0	1.3	0.48	-
	5	2.5	0.36	48.8
45	10	2.7	0.30	52.9
	25	2.8	0.20	55.1
	50	3.2	0.17	59.5
	0	1.1	0.61	-
	5	2.1	0.41	43.7
50	10	2.3	0.39	48.8
	25	2.4	0.33	51.2
	50	2.8	0.31	57.8

The effect of chemically stable surface active inhibitors is to increase the energy of activation and to decrease the surface area available for corrosion [35]. The results in Table 4 indicate that the value of activation energy (E_a) in 0.5 M NaOH solution containing inhibitor is greater than that without the inhibitor. The increase in the activation energies with the increasing concentration of the inhibitor is attributed to physical adsorption of inhibitor molecules on the metal surface with an appreciable increase in the adsorption process of the inhibitor on the metal surface with the increase in the concentration of the inhibitor [36]. The adsorption of the inhibitor molecules on the surface of the metal blocks the charge transfer during the corrosion reaction, thereby increasing the activation energy [37].

The adsorption of the inhibitor on the electrode surface leads to the formation of a physical barrier between the metal surface and the

corrosion medium, which reduces the metal reactivity in the electrochemical reactions of corrosion. The decrease in the inhibition efficiency of MAMT with the increase in temperature can be attributed to an appreciable decrease in the adsorption of the inhibitor on the metal surface with increase in temperature and corresponding increase in corrosion rate, because greater area of the metal gets exposed to the corrosion medium.

Table 4. Activation parameters for the corrosion of for the corrosion of 6061/Al - 15 (vol-%) SiC$_{(p)}$ composite in 0.5 M NaOH solution containing different concentrations of MAMT.

Conc. of inhibitor (ppm)	E_a (kJ mol^{-1})	ΔH_a (kJ mol^{-1})	$-\Delta S_a$ (J mol^{-1} K^{-1})
0	6.73	4.13	192.55
5	10.72	8.12	186.42
10	11.40	8.80	184.96
25	12.92	10.32	181.21
50	18.61	16.01	163.55

The entropy of activation values in the absence and presence of inhibitor are negative. This implies that the activated complex in the rate-determining step represents an association rather than dissociation, resulting in a decrease in randomness on going from reactants to activated complex [10]. The entropy of activation values are less negative for inhibited solutions than that for the uninhibited solutions. This suggests that an increase in randomness occurs while moving from the reactants to the activated complex in the presence of the inhibitor. This might be the result of the adsorption of organic inhibitor molecules from the alkaline medium, which could be regarded as a quasi substitution process between the inhibitor compound in the aqueous phase and water molecules at electrode surface [38]. In this situation, the adsorption of organic inhibitor is accompanied by desorption of water molecules from the surface. Thus, the increase in entropy of activation is attributed to the increase in solvent entropy [39].

3.4. Adsorption behavior

Organic corrosion inhibitors are known to decrease the metal dissolution via adsorption on the metal/corrodent interface to form a protective film which separates the metal surface from the corrosive medium. The adsorption route is usually regarded as a substitution process between the organic inhibitor in the aqueous solution [Inh$_{(sol)}$]

and water molecules adsorbed at the metal surface [H$_2$O$_{(ads)}$] as given below [40]:

$$\text{Inh}_{(sol)} + \chi \text{H}_2\text{O} \leftrightarrow \text{Inh}_{(ads)} + \chi \text{H}_2\text{O} \qquad (10)$$
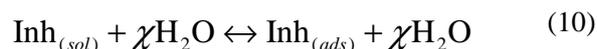
where χ represents the number of water molecules replaced by one molecule of a adsorbed inhibitor. The adsorption bond strength is dependent on the composition of the metal, corrodent, inhibitor structure, concentration and orientation as well as temperature. Basic information on the interaction between the inhibitor and composite surface can be provided by adsorption isotherm. The degree of surface coverage (θ) in the presence of different concentrations of inhibitor was evaluated from potentiodynamic polarization measurements. The data were applied to various isotherms including Langmuir, Temkin, Frumkin and Flory-Huggins isotherms. By far, the best fit was obtained with the Langmuir adsorption isotherm. The Langmuir Adsorption isotherm could be represented by the equation:

$$\frac{C}{\theta} = C + \frac{1}{K} \qquad (11)$$

where K is the adsorption/desorption equilibrium constant, C is the corrosion inhibitor concentration in the solution, and θ is the surface coverage, which is calculated using Eq 12:

J. Mater. Environ. Sci. 2 (4) (2011) 387-402
ISSN : 2028-2508

Kumari et al.

$$\theta = \frac{\eta}{100} \tag{12}$$

where η is the inhibition efficiency as calculated using Eq. 1. Taking logarithm on both the sides of Eq. 11., Eq 13. is obtained.

$$\log\left(\frac{C}{\theta}\right) = \log C - \log K \tag{13}$$

The plot of log (C/θ) versus log C gives a straight line with intercept equal to –log K as shown in Fig. 6, but the slopes show deviation from the value of unity as would be expected for the ideal Langmuir adsorption isotherm equation. This deviation from unity may be due to the interaction among the adsorbed species on the metal surface. The Langmuir isotherm equation is based on the assumption that adsorbed molecules do not interact with one another, but this is not true in the case of organic molecules having polar atoms or groups which are adsorbed on the cathodic and anodic sites of the metal surface. Such adsorbed species may interact by mutual repulsion or attraction. Similar results have been reported by Sethi et al [41].

The thermodynamic parameter, standard free energy of adsorption, (ΔG^0_{ads}) is calculated from the thermodynamic equation:

$$K = \frac{1}{55.5} \exp\left(\frac{-\Delta G^0_{ads}}{RT}\right) \tag{14}$$

where K is the equilibrium constant for the adsorption/desorption process, 55.5 mol dm^{-3} is the molar concentration of water in the solution, T is temperature and R is ideal gas constant.

Standard enthalpy of adsorption (ΔH^0_{ads}) and standard entropies of adsorption (ΔS^0_{ads}) were obtained from the plot of (ΔG^0_{ads}) versus T according to the thermodynamic basic equation

$$\Delta G^0_{ads} = \Delta H^0_{ads} - T\Delta S^0_{ads} \tag{15}$$

The values of standard free energy of adsorption (ΔG^0_{ads}), standard enthalpy of adsorption (ΔH^0_{ads}) and standard entropy (ΔS^0_{ads}) for the adsorption process are listed in Table 5.

.
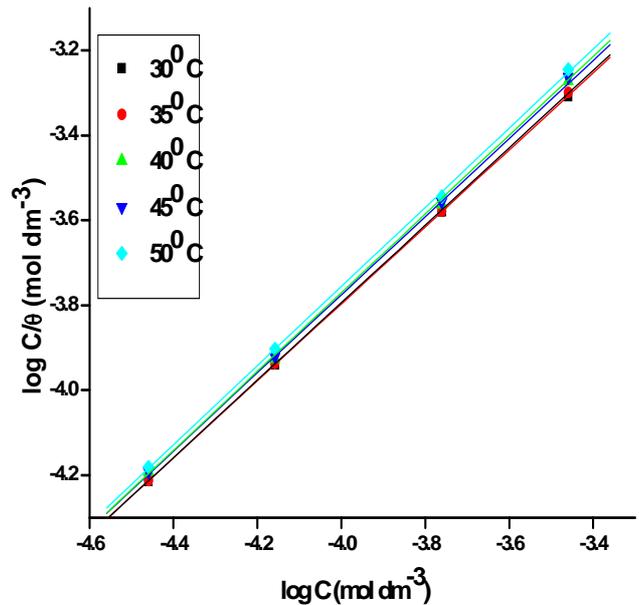
Figure 6. Langmuir adsorption isotherms for the adsorption of MAMT on the composite.

The adsorption heat could be approximately regarded as the standard adsorption heat (ΔH^0_{ads}) under the experimental conditions [42]. The negative sign of ΔH^0_{ads} in NaOH solution indicates that the adsorption of inhibitor molecule is an exothermic process. Generally, an exothermic adsorption process signifies either physisorption or chemisorptions while endothermic process is attributable unequivocally to chemisorption [43]. Typically, the enthalpy of physisorption process is lower than that 41.86 kJ mol^{-1}, while the enthalpy of chemisorptions process approaches to 100 kJ mol^{-1} [44]. In the present study, the value of ΔH^0_{ads} is -24.35 kJ mol^{-1}, which indicates that the adsorption of MAMT on 6061 Al/SiC$_p$ involves physisorption phenomenon.

Table 5. Thermodynamic parameters for the adsorption of MAMT on 6061/Al - 15 (vol-%) SiC$_{(p)}$ composite in 0.5 M NaOH solution containing at different temperatures.

Temp (°C)	$-\Delta G^0_{ads}$ (kJ mol$^{-1)}$)	$-\Delta H^0_{ads}$ (kJ mol^{-1})	$-\Delta S^0_{ads}$ (J mol^{-1} K^{-1})
30	11.1		
35	11.0		
40	10.7	24.4	43.6
45	10.5		
50	10.3		

The negative values of ΔG^0_{ads} indicate the spontaneity of the adsorption process and stability of the adsorbed layer on the metal surface. Generally the values of ΔG^0_{ads} less negative than -20 kJ mol^{-1} are consistent with physisorption, while those more negative than -40 kJ mol^{-1} involve chemisorptions [45]. The calculated values of ΔG^0_{ads} obtained in this study range between -10.28 and -11.12 kJ mol^{-1} indicating physical adsorption behavior of MAMT on the aluminium composite surface. Also when the inhibition efficiency (η) decreases with the increase in temperature as observed in this study, it points straight to physical adsorption mechanism.

The ΔS^0_{ads} values in the presence of the inhibitor are negative, indicating that an increase in orderliness takes place on going from the free state to the adsorbed state of the inhibitors. This might be attributed to the orderly adsorption of the inhibitor molecules from a chaotic state of the freely moving molecules in the solution [46].

3.5. Effect of the immersion time

Electrochemical impedance spectroscopy is a rapid and useful technique to evaluate the performance of the organic-coated metals because they do not significantly disturb the system and it is possible to follow it overtime. Therefore more reliable results can be obtained from this technique and

also it is possible to characterize the surface modification i. e., formation and growth of the inhibitor film [47]. Immersion time experiments were carried out in 0.5 M NaOH solution containing 50 ppm of MAMT for 360 minutes at 30 °C and Nyquists plots were recorded at every 5 min during the initial 30 min, and then every 30 min afterward. The obtained results showed that the increase in immersion time increased the size of the capacitive loop and reaching a maximum in 120 min. After that a slight decrease in the R_p value is observed, which may be due to the formation of some defects on the film leading to the access of aggressive ions to the metal/inhibitor interface.

In Fig. 7 the variation of both R_p and C_{dl} with the immersion time recorded for 0.5 M NaOH solution are shown graphically. It is obvious from the figure that R_p values increased from 4.739 ohm cm^2 to 5.789 ohm cm^2 during the initial 120 min. At the same time, C_{dl} values decreased up to 120 min and thereafter a slight increase is observed. These results indicate that the adsorption and orientation of MAMT on the surface of the composite, changes with time. Considering that adsorption is essentially controlled by electrostatic attraction, as the immersion time increases, more MAMT will be adsorbed on the surface helping to the formation of the inhibitor layers.

J. Mater. Environ. Sci. 2 (4) (2011) 387-402
ISSN : 2028-2508

Kumari et al.
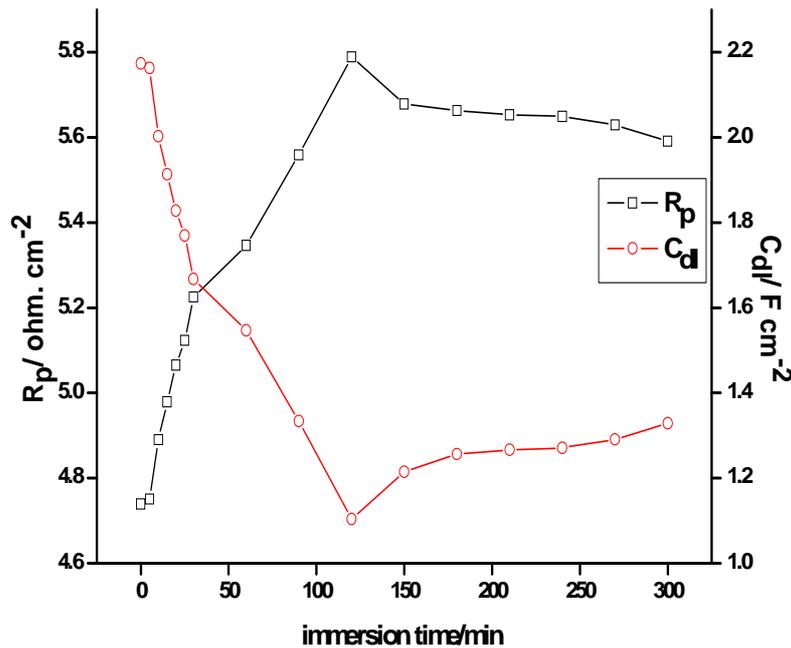
Figure 7. The dependence of R_p and C_{dl} on the immersion time for the corrosion 6061/Al - 15 (vol-%) SiC$_{(p)}$ composite in 0.5 M NaOH in the presence of 50 ppm MAMT at 30 °C.

3.6. Inhibition mechanism

It is known that high inhibition efficiencies on aluminum surface are obtained in the acid medium, whereas only nominal inhibition efficiencies are schieved in alkaline solutions. This may be attributed to the high negative potential of aluminum in the alkaline solution which may not be favorable for the adsorption of the organic compounds [48]. However in this case using MAMT as corrosion inhibitor for 6061/Al - 15 (vol-%) SiC$_{(p)}$ composite in 0.5 M sodium hydroxide, about 70% corrosion inhibition efficiency is achieved. The good inhibition efficiency of MAMT is attributed to the strong adsorption of inhibitor species on the composite metal surface through the active centers, nitrogen and sulfur atoms.

In alkaline solution the corrosion of aluminum could be explained by taking into account of the passive film, covering the surface of aluminum. In the strong alkaline medium, as used in the present study, the surface film readily dissolves exposing the underlying aluminum atoms, resulting in the dissolution of aluminum atoms and gradual removal of these atoms through the formation of hydroxide, Al(OH)$_3$ (Eq 16). Al(OH)$_4^-$, that goes into the solution, leaving a

bare metal site ready for another dissolution process [49,50].

$$Al(m) + 3(OH)^- \rightleftharpoons Al(OH)_3 \qquad (16)$$

$$Al(OH)_3 + OH^- \rightleftharpoons Al(OH)_4^- \qquad (17)$$
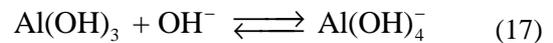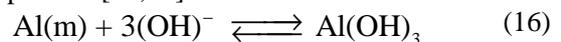
The principal cathodic process is the reduction of water molecules to produce H$_2$ gas according to:

$$H_2O_{(surface)} + e^- \rightleftharpoons H + OH^- \qquad (18)$$

$$H + H_2O_{(surface)} + e^- \rightleftharpoons H_2 + OH^- \quad (19)$$
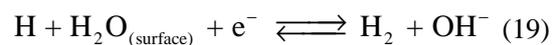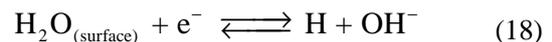
The hydrogen overvoltage on aluminum is low, and therefore there is intense evolution of hydrogen when aluminum corrodes in NaOH solution. The inhibitor may affect either of the anodic and cathodic processes or both of them.

In NaOH solution MAMT exits in the anionic form by the deprotonation of –SH group. Presence of methyl group in MAMT molecule with + R (resonance) and + I (inductive) effects has a marked effect on the inhibition efficiency of the triazole molecule. This would donate charge through hyper-conjugation and by the inductive effect thus concentrating the charge density on nitrogen and sulfur atoms, thereby increasing their adsorption at the anodic sites of the metal. The

inhibitor anions with high charge density may also compete with anions such as OH⁻ ions (Eq. 17) and preferentially get adsorbed at the anodic sites of the metal surface. Adsorption of the inhibitor at the metal surface replaces the water molecules within the electrical double layer to produce less pronounced dielectric effect [51] and thus holds up the reaction of surface water molecules according to Eq. (18) and Eq. (19), thus the rate of hydrogen evolution is reduced, thereby effecting the cathodic reactions.

3.7. Scanning Electron Microscopy

In order to evaluate the surface morphology of the composite surface in contact with alkaline solution, a superficial analysis was carried out. The SEM micrograph of the corroded specimen after 1 hour of immersion in 0.5 M NaOH solution is shown in Fig 8(a).The faceting seen in the figure is due to the attack of aggressive hydroxide ions on the composite sample, causing more or less uniform corrosion. Fig 8(b) depicts the SEM of the specimen after 1 hour of immersion in 0.5 M NaOH solution in the presence of 50 ppm MAMT. It can be seen that the flakes on the surface of the specimen are reduced when compared with the micrograph given in Fig 8(a). The specimen surface can be observed to be covered with a thin layer of the inhibitor molecules, giving protection against corrosion.
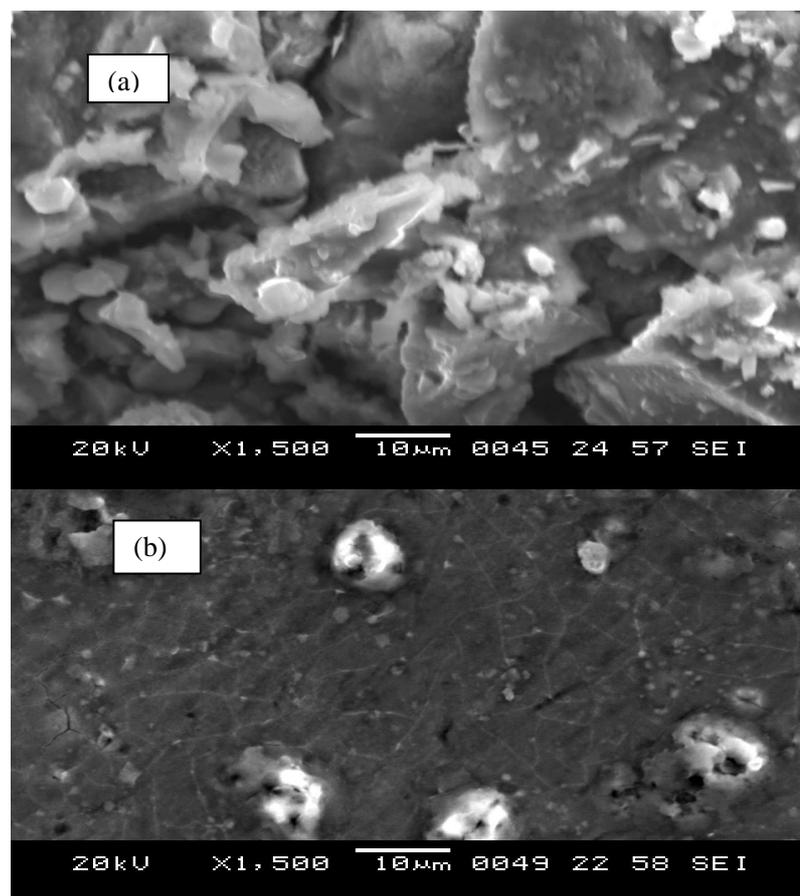
Figure 8. SEM images of the surfaces of 6061/Al - 15 (vol-%) SiC$_{(p)}$ after immersion for 1 h in 0.5 M NaOH solution at 30 °C (a) in the absence of MAMT (b) in the presence of 50 ppm MAMT.

Conclusion

Potentiodynamic polarization and electrochemical impedance methods used to evaluate the ability of MAMT to inhibit corrosion of 6061/Al - 15 (vol-%) SiC$_{(p)}$ composite in 0.5 M NaOH. The principal conclusions are

- MAMT acts as a good inhibitor for the corrosion of composite in 0.5 M NaOH solution.
- The inhibition efficiency increases with the increase in inhibitor concentration and decreases with the increase in temperature of the medium.
- MAMT behaves predominantly as a cathodic inhibitor.
- The adsorption of MAMT on the composite metal surface is through physisorption, obeying Langmuir's adsorption isotherm model.
- The negative values of ΔG^0_{ads} obtained indicate the spontaneous adsorption of MAMT on the composite surface.
- The inhibition efficiency obtained from potentiodynamic polarization and EIS techniques are in reasonably good agreement.

References

1. Candan, S., Biligic, E. *Mater. Lett.* 58 (2004) 2787.
2. Bakkar, A., Neubert, V. *Corros. Sci.* 49 (2007) 1110.
3. Griffiths, A.J., Turnbull, A. *Corros. Sci.* 36 (1994) 23.
4. Trowsdale, A.J., Noble, B., Harris, S.J., Gibbins, I.S.R., Thompson, G.E., Wood, G.C. *Corros. Sci.* 2 (1996) 177.
5. Talati, J.D., Modi, R.M. *Corros. Sci.* 19 (1979) 35.
6. Muller, B. *Corros. Sci.* 43 (2001) 1155.
7. Henryk, S., Martin, M.D.J. *Corros. Sci.* 12 (1992) 1967.
8. Bereket, G., Pinarbasi, A. *Corros. Eng. Sci. Technol.* 39 (2004) 308.
9. Zheludkevich, M.L., Yasakau, K.A., Poznyak, S.K., Ferreria, M.G.S. *Corros. Sci.* 47 (2005) 3368.
10. Abdallah, M. *Corros. Sci.* 46 (2004) 1981.
11. Pinto, G.M., Nayak, J., Shetty, A.N. *Mater. Chem. Phy.* 125 (2011) 628.
12. Kumari, P.D.R., Nayak. J., Shetty, A.N. *J. Coat. Tech. Res.* (2011) DOI 10.1007/s11998-011-9341-2
13. Suma, A.R., Padmalatha., Nayak, J., Shetty, A.N. *J. Metal. Mater. Sci.* 47 (2005) 51.
14. Bektas, H., Karaali, N., Sahin, D., Demirbas, A., Karaoglu, S.A. *Molecules.* 15 (2010) 2427.
15. Poornima, T., Nayak, J., Shetty, A.N. *J. Appl. Electrochem.* 41 (2011) 223.
16. Gadag, R.V. Doctoral dissertation; University of Mysore; India (1986).
17. Fontana, M.G. (1987) Corrosion Engineering. 3rd edn. McGraw-Hill, Singapore
18. Ferreira, E.S., Gianocomelli, C., Giacomelli, F.C., Spinelli, A. *Mater. Chem. Phy.* 83 (2004), 129.
19. Li, W.H., He, Q., Pei, C.L., Hou, B.R. *J. Appl. Electrochem.* 38 (2008) 289.
20. McCafferty, E., Hackerman, N. *J. Electrochem. Soc.* 119 (1972) 999.
21. Amin, M.A., Abd El-Rehim, S.S., El-Sherbini, E.E.F., Bayyomi, R.S. *Electrochim. Acta.* 52 (2007) 3588.
22. Mansfeld, F., Lin. S., Kim, K., Shih, H. *Corros. Sci.* 27 (1987) 997.
23. Mansfeld, F., Lin, S., Kim, S., Shih, H. *Mater. Corros.* 39 (1988) 487.
24. Brett, C.M.A. *J. Appl. Electrochem.* 20 (1990) 1000.
25. Brett, C.M.A. *Corros. Sci.* 33 (1992) 203.
26. Wit, J.H., Lenderink, H.J.W. *Electrochim. Acta.* 41 (1996) 1111.
27. Lenderink, H.J.W., Linden, M.V.D., De Wit, J.H.W. *Electrochim. Acta.* 38 (1993) 1989.
28. Macdonald, D.D., Real, S., Smeldley, S.I. *J. Electrochem. Soc.* 135 (1988) 2410.
29. Jutner, K. *Electrochim. Acta.* 35 (1990) 1501.
30. Mansfeld, F., Tsai, C.H., Shih, H. (1992) Computer modeling in corrosion. In: Munn RS (ed.), ASTM, Philadelphia
31. Hsu, C.H., Mansfeld, F. *Corrosion.* 57 (2001) 747.

J. Mater. Environ. Sci. 2 (4) (2011) 387-402
Kumari et al.

ISSN : 2028-2508

32. Bentiss, F., Traisnel, M., Lagrenee, M. *Corros. Sci.* 42 (2000) 127.
33. Bentiss, F., Lebrini, M., Lagrenée, M. *Corros. Sci.* 47 (2005) 2915.
34. Schorr, M., Yahalom, J. *Corros. Sci.* 12 (1972) 867.
35. Antropov, L.I. Corros. Sci. 7 (1967) 607.
36. Ashassi-Sorkhabi, H., Shaabani, B., Seifzadeh, D. *Appl. Surf. Sci.* 239 (2005) 154.
37. Osman, M.M., El-Ghazawy, R.A., Al-Sabagh, A.M. *Mater. Chem. Phy.* 80 (2003) 55.
38. Sahin, M., Bilgic, S., Yilmaz, H. *Appl. Surf. Sci.* 195 (2002) 1.
39. Ateya, B., El-Anadouli, B.E., El-Nizamy, F.M. *Corros. Sci.* 24 (1984) 509.
40. Oguzie, E.E., Njoku, V.O., Enenebeak, C.K., Akalezi, C.O., Obi, C. *Corros. Sci.* 50 (2008) 3480.
41. Sethi, T., Chaturvedi, A., Upadhyay, R.K., Mathur, S.P. *J. Chil. Chem. Soc.* 52 (2007) 1206.
42. Singh, A.K., Quraishi, M.A. *Corros. Sci.* 52 (2010) 152.
43. Durnie, W., Marco, R.D., Jefferson, A., Kinsella, B. *J. Electrochem. Soc.* 146 (1999) 1751.
44. Martinez, S., Stern, S.I. *Appl. Surf. Sci.* 199 (2002) 83.
45. Umoren, S.A., Ebenso, E.E., Okafor, P.C., Ekpe, U.J., Ogbobe, O. *J. Appl. Polym. Sci.* 103 (2007) 2810.
46. Libin, T., Guannan, M., Guangheng, L. *Corros. Sci.* 45 (2003) 2251.
47. Solmaz, R., Kardas, G., Culha, M., Yazici. B., Erbil, M. *Electrochim. Acta.* 53 (2008) 5941.
48. Desai, M.N., Desai, S.M. *Corros. Sci.* 10 (1970) 233.
49. Lorenz, W.J., Mansfeld, F. *Corros. Sci.* 21 (1981) 647.
50. Doche, M.L., Rameau, J.J., Durand, R., Novel-Cattin, F. *Corros. Sci.* 41 (1999) 805.
51. Yazdad, A.R., Shahrabi, T., Hosseini, M.G. *Mater. Chem. Phy.* 109 (2008) 199.